Fırat Üniversitesi Deneysel ve Hesaplamalı Mühendislik Dergisi

Akım Gözlemi Olmayan Havzalarda Sentetik Birim Hidrograf Yöntemleri ve CBS Kullanılarak Taşkın Debilerinin Tahmini

Erdal KESGİN[1]*

[1]İnşaat Mühendisliği Bölümü, İnşaat Fakültesi, İstanbul Teknik Üniversitesi, İstanbul, Türkiye.
[1]kesgine@itu.edu.tr

Geliş Tarihi: 24.02.2025
Kabul Tarihi: 22.04.2025
Düzeltme Tarihi: 26.03.2025
doi: https://doi.org/10.62520/fujece.1645774
Araştırma Makalesi

Alıntı: E. Kesgin, ’’Akım gözlemi olmayan havzalarda sentetik birim hidrograf yöntemleri ve cbs kullanılarak taşkın debilerinin tahmini”, Fırat Üni. Deny. ve Hes. Müh. Derg., vol. 4, no 2, pp. 375-392, Haziran 2025.

Öz

Taşkın, bir akarsuyun çeşitli nedenlerle yatağından taşarak çevresindeki arazi, yerleşim alanları, altyapı tesisleri ve ekosistem üzerinde oluşturduğu olumsuz etkiler olarak tanımlanabilir. Havza ölçeğinde, özellikle akım gözlem istasyonlarının bulunmadığı durumlarda, taşkın analizleri için yağış-akış ilişkileri için hidrograflar oluşturulmalıdır. Bu çalışmada, İstanbul, Sarıyer ilçesinde yer alan ve büyük ölçüde ormanlık niteliğindeki bir alt havza için sentetik hidrografların oluşturulması, yağış-akış ilişkilerinin analiz edilmesi ve farklı tekerrür aralıkları için taşkın debilerinin hesaplanması amaçlanmıştır. Ekstrem yağış analizleri kapsamında, Normal, Log-Normal, Log-Pearson Tip III ve Gumbel olasılık dağılım fonksiyonları kullanılarak çeşitli tekerrür aralıkları (T = 2, 5, 10, 25, 50, 100 yıl) için 24 saatlik maksimum yağış değerleri hesaplanmıştır. Log-Pearson Tip III yöntemiyle elde edilen yağış değerlerinin daha yüksek olduğu belirlenmiş ve taşkınların ekstrem doğası göz önüne alındığında, debi hesaplamalarında bu yöntemin kullanılması tercih edilmiştir. Çalışmanın ikinci aşamasında, havzanın fiziksel özellikleri ve boyutsuz birim hidrograf koordinatları kullanılarak, DSI, Mockus ve Snyder birim hidrograf yöntemleri aracılığıyla çeşitli tekerrür aralıkları için havzaya özgü taşkın hidrografları üretilmiştir. Sonuçlar, DSI ve Mockus yöntemlerinin birbirine yakın ve yüksek pik debi değerleri ürettiğini (T = 100 yıl için Q_{max} sırasıyla 67,44 ve 63,76 m³/s), buna karşın Snyder yönteminin daha düşük pik debi değerleri (T = 100 yıl için Q_{max} = 32,17 m³/s) ancak daha uzun süreli bir hidrograf oluşturduğunu ortaya koymuştur. Genel olarak, DSI ve Mockus yöntemlerinin, ormanlık ve nispeten küçük havzalarda (≈10 km²) taşkın analizlerinde kullanılacak hidrografın oluşturulması açısından daha uygun olduğu sonucuna varılmıştır. Bu çalışma, İstanbul'un kentleşen bir bölgesinde, ormanlık alanların hâkim olduğu ölçüm istasyonu bulunmayan bir havza için özel olarak uyarlanmış üç yaygın sentetik birim hidrograf yönteminin karşılaştırmalı bir değerlendirmesini sunarak, veri yetersizliği yaşanan bölgelerde hidrolojik modelleme konusunda literatüre katkı sağlamaktadır.

Anahtar kelimeler: Coğrafi bilgi sistemleri (CBS), Sentetik birim hidrograf, Taşkın, Mockus, Snyder

*Yazışılan Yazar

İntihal Kontrol: Evet – Turnitin
Şikayet: fujece@firat.edu.tr

Firat University Journal of Experimental and Computational Engineering

Flood Discharge Estimation in Ungauged Basins Using Synthetic Unit Hydrographs and GIS

Erdal KESGİN [1*]

[1]Civil Engineering Department, Faculty of Civil Engineering, Istanbul Technical University, Istanbul, Türkiye.
[1]kesgine@itu.edu.tr

Received: 24.02.2025
Accepted: 22.04.2025
Revision: 26.03.2025
doi: https://doi.org/10.62520/fujece.1645774
Research Article

Citation: E. Kesgin,“ Flood discharge estimation in ungauged basins using synthetic unit hydrographs and gıs”, Firat Univ. Jour.of Exper. and Comp. Eng., vol. 4, no 2, pp. 375-392, June 2025.

Abstract

Flooding refers to the adverse effects caused by rivers overflowing their banks due to various reasons, affecting surrounding land, residential areas, and infrastructure. At the watershed scale, particularly in cases where flow monitoring stations are absent, hydrographs must be generated to analyze rainfall-runoff relationships for flood assessments. This study aims to generate synthetic hydrographs, analyze rainfall-runoff relationships, and estimate flood discharges for different return periods in a predominantly forested sub-watershed located in the Sarıyer district of Istanbul. The study analyzed extreme rainfall by calculating 24-hour maximum values for return periods of 2 to 100 years using four common probability distribution functions: Normal, Log-Normal, Log-Pearson Type III, and Gumbel. Among these methods, Log-Pearson Type III yielded higher rainfall values, and given the extreme nature of floods, it was preferred for discharge calculations. In the second stage of the study, flood hydrographs specific to the watershed were generated for different return periods using the DSI, Mockus, and Snyder unit hydrograph methods, incorporating watershed physical characteristics and dimensionless unit hydrograph coordinates. The results indicated that the DSI and Mockus methods produced similar and higher peak discharge values (Q_{max} = 67.44 and 63.76 m³/s, T=100 years), whereas the Snyder method resulted in lower peak discharge (Q_{max} = 32.17 m³/s for T = 100 years) but a longer hydrograph duration. Overall, it was concluded that the DSI and Mockus methods are more suitable for flood analysis in forested and relatively small watersheds (≈10 km²) due to their effectiveness in generating hydrographs for flood assessments. This study contributes to the literature by offering a comparative evaluation of three widely used synthetic unit hydrograph methods, specifically tailored for a forest-dominated ungauged basin in an urbanizing region of Istanbul, providing actionable insights for flood estimation in data-scarce, forested urban catchments.

Keywords: Geographical information systems (GIS), Synthetic unit hydrograph, Flood, Mockus, Snyder

[*]Corresponding author

1. Introduction

Flooding is a natural phenomenon in which a river overflows its banks due to various factors, causing damage to surrounding land, settlements, infrastructure, and living organisms while disrupting the economic and social life of the affected region [1]. Factors such as climate change, unplanned urbanization, unauthorized interventions in riverbeds, degradation of river basins, improper use of floodplains, and inadequate infrastructure for water flow in road and railway crossings further exacerbate the impacts of floods. Human influence plays a significant role in flood occurrence. In the absence of natural meteorological and geological conditions, flooding is unlikely to occur without natural or anthropogenic triggers. However, human interventions are a decisive factor in transforming floods into disasters. For instance, uncontrolled construction in floodplains, unauthorized urbanization in upstream areas, deforestation, vegetation loss, and improper land use are among the key contributing factors. Floods—frequently observed in Türkiye— rank second after earthquakes in terms of economic losses caused by natural disasters [2]. Compared to earthquakes, predicting the potential impacts of floods is relatively easier. However, it is not possible to determine the exact extent of the damage they may cause. Estimating flood discharges enables the modeling of flood scenarios and helps identify appropriate mitigation strategies. Therefore, the magnitude of floods can be scientifically calculated through statistical analyses based on available hydrometeorological data, allowing the development of flood scenarios with different return periods.

A river basin is defined as a system that transforms incoming rainfall into runoff. Therefore, for a given river basin, rainfall serves as the input parameter, while runoff is considered the output dependent on this rainfall. When there is a lack of flow measurements over a certain period or an absence of any flow observations within a river basin, estimating runoff values based on rainfall becomes a fundamental motivation for analyzing the basin as a system. However, due to the complex nature of the rainfall-runoff relationship in river basins, the system is often simplified through certain assumptions, leading to the development of a mathematical model [3]. During the planning of hydraulic structures or the construction of river engineering projects, it is essential to determine flood peaks that may occur at various return periods (e.g., T = 10, 100, 500 years). The most commonly used methods for estimating flood peaks include: (i) Statistical approaches based on streamflow observations to calculate flood peak and duration, and (ii) Methods utilizing rainfall data and unit hydrographs to estimate flood peaks and their durations. If a sufficient number of streamflow measurements are available for the watershed, statistical methods can yield reliable results for flood discharge estimation. However, in many rainfall-dominated regions, rainfall-runoff data are often unavailable. Consequently, synthetic unit hydrographs have been developed to address this limitation.

Sönmez et al., (2012) [4] applied the Snyder, Kirpich, Mockus, and Soil Conservation Service (SCS) methods to estimate flood discharge for eight streams in Istanbul. They reported that the Snyder method yielded higher discharge values; however, they also noted that this method is directly related to watershed area and geometric shape. Consequently, an increase in flood discharge was observed as the watershed area increased. Kumanlıoğlu and Ersoy (2018) [5] estimated flood discharges for various return periods in the Kızıldere stream, a tributary of the Gediz River, using the SCS and Mockus methods. They emphasized the necessity of determining these flood hydrographs to minimize potential loss of life and property, particularly in watersheds with high agricultural productivity. Bantchina and Gündoğdu (2021) [6] analyzed flood discharges and watershed characteristics for the Nilüfer Dam Basin (Türkiye) using Geographic Information Systems (GIS) and various synthetic unit hydrograph methods, including the DSI, Mockus, and the Snyder methods. Their results indicated that the highest peak discharge value was obtained using the DSI method (Q_p=4.40 m³/s/mm), while the lowest was derived from the Mockus method (Q_p=3.75 m³/s/mm). They highlighted the necessity of employing synthetic unit hydrograph methods in stations lacking direct flow measurements.

In the presented study, flood hydrographs corresponding to different return periods were determined for a sub-basin in Sarıyer, Istanbul, where no streamflow measurement data are available. These hydrographs were generated using synthetic unit hydrographs, including the DSI Synthetic Method, Mockus Method, and Snyder Method. As part of the analysis, a frequency analysis was conducted using the highest value among the annual maximum daily (24-hour) precipitation records, and the best-fitting probability distribution function was identified to derive daily maximum precipitation values for different return periods. These precipitation values were then used as the primary input data for constructing synthetic unit hydrographs. Unlike many prior studies centered on rural or agricultural areas, this research examines a forested sub-basin in a rapidly urbanizing region. This setting offers a unique opportunity to evaluate the reliability of synthetic hydrograph methods in the complete absence of flow measurements. Furthermore, the study integrates high-resolution GIS data and evaluates method performance across a full range of return periods, which enhances its practical relevance for urban flood risk planning.

The main objective of the present study is to estimate flood discharges in a small, ungauged, forest-dominated sub-catchment in Istanbul's Sarıyer district using three widely applied synthetic unit hydrograph methods DSI, Mockus, and Snyder. Even though synthetic methods have been used in many basins of Türkiye, comparative assessments for forested urban basins are limited in the literature. This study closes that gap by evaluating the performance of each method under different return periods, giving insight into their dependability in hydrologically similar basins. The results enhance not only knowledge on rainfall-runoff modeling in data-poor areas but also inform real-world practice among hydrologists and engineers designing drainage and flood control systems for rapidly urbanizing, topographically heterogeneous watersheds

2. Materials and Methods

2.1. Study area and dataset

The study area encompasses a sub-basin located within the boundaries of Sarıyer district on the European side of Istanbul. This region, which covers an area of approximately 10 km², is a mostly forested area located to the west of the Sarıyer district center, south of the Zekeriyaköy district and west of the Bahçeköy district. A map generated using a 5-meter resolution Digital Elevation Model (DEM) provides a detailed representation of the study area and is presented in Figure 1. The elevation of the basin ranges from 2 to 234 meters, with an average elevation of 109.5 meters. While higher altitude values are observed in the northern parts, the altitude decreases towards the south. To analyze the land use and land cover (LULC) of the study area, Landsat-8 satellite images from 2023 were downloaded at a 10×10 m resolution using the Sentinel-2 Land Cover Explorer. According to the findings, approximately 80% of the basin area is forested and the remaining part is built area (Figure 1.). An analysis of the climatic characteristics of the study area, based on maps prepared by the Republic of Turkey Ministry of Environment, Urbanization, and Climate Change, reveals that the region falls within a humid to semi-humid climate zone according to various classification methods, including those of Aydeniz, Erinç, and Thornthwaite. This indicates that the area experiences mild winters and hot summers, exhibiting characteristics similar to the Mediterranean climate. In the calculation of flood discharges, the curve number (CN) of the basin was determined to be 55 by considering the basin's vegetation cover and geological structure together.

In this study, annual maximum rainfall data from the Turkish State Meteorological Service, specifically from the Sarıyer station, were obtained (Figure 2.). Using the daily maximum rainfall data, extreme rainfall values were calculated using probability distribution functions commonly employed in the literature, such as Normal, Log-Normal, Log-Pearson Type III, and Gumbel. The calculated extreme rainfall values were used as input parameters for generating synthetic unit hydrographs across various return periods.

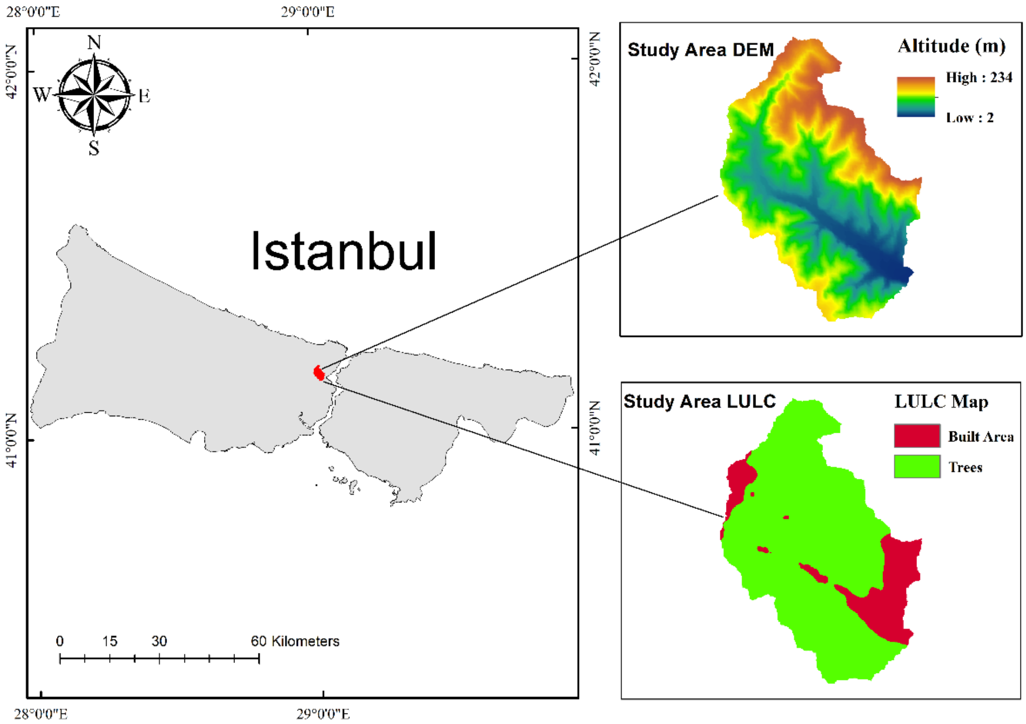

Figure 1. Study area DEM and land use land cover map (LULC)

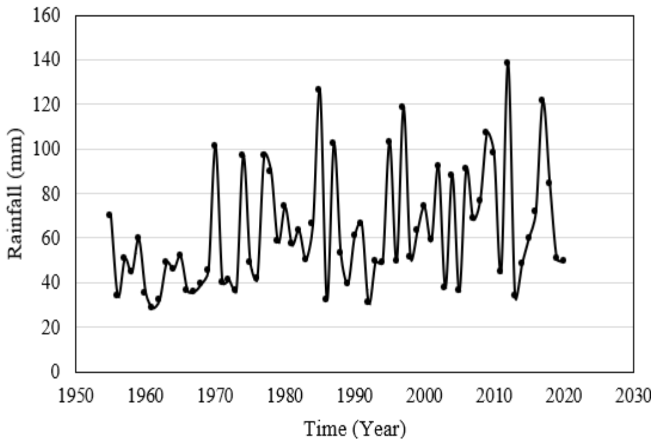

Figure 2. Annual maximum 24-hour observed precipitation at Sarıyer Meteorological station

2.2. Probability density functions

The irregularity of rainfall leads to many hydrological variables exhibiting the characteristics of random variables. Due to the availability of long-term rainfall records, statistical methods have been employed in the calculation of extreme rainfall values. In this study, extreme rainfall values were calculated using probability distribution functions that are frequently used in the literature, including Normal, Log-Normal, Log-Pearson Type III, and Gumbel. The probability distribution functions and their parameters used for extreme rainfall analysis in this study are summarized in Table 1.

For the Normal distribution, the possible rainfall values for specific return periods (T) are expressed in Equation 4 in Table 1. The three key parameters are the arithmetic mean (μ_x), standard deviation (σ_x), and frequency factor (K_T). While the mean and standard deviation are obtained from the dataset, the frequency factor is calculated using Equation 3. The "w" parameter in Equation 3 is calculated based on the exceedance probability of the return period (p = 1/T), as presented in Equation 2.

The Log-Normal distribution is expressed as the distribution of a random variable whose logarithm follows a normal distribution. The necessary operations to calculate the likely extreme rainfall for a given return period are equivalent to those of the Normal distribution. However, it is important to note that in this case, the "x" values must be processed as "logx."

The Gumbel distribution is widely used in hydrological studies due to its success in modeling extreme data [7-8]. It estimates rainfall values based on the mean, standard deviation, and a modified frequency factor (K_T) defined specifically for extreme value distributions [9-10].

The Log-Pearson Type III distribution is frequently utilized in estimating floods for different return periods. Several studies have emphasized that this distribution is recommended for flood estimation because it accounts for the skewness in rainfall data [9-10]. The frequency factor (k) for the Log-Pearson Type III distribution is used as shown in Equation 14 and is read from various tables depending on the return periods and C_s value [11].

Table 1. Probability Density Functions and calculation formulas

PDF	Equations	
Normal	$f(x)=\frac{1}{\sqrt{2\pi_x^{2}}}\exp\left[-\frac{1}{2}\left(\frac{x-\mu_x}{\sigma_x}\right)^2\right]$	(1)
	$w=\sqrt{\ln\left(\frac{1}{p^2}\right)}$	(2)
	$K_T=w-\frac{\left[2.515517+\left(0.802853\times w\right)+\left(0.010328\times w^2\right)\right]}{\left[1+\left(1.432788\times w\right)+\left(0.189269\times w^2\right)+\left(0.001308\times w^3\right)\right]}$	(3)
	$X_T=\mu_X+\left(K_T\times\sigma_X\right)$	(4)
Log Normal	$f(x)=\frac{1}{x\sigma_y\sqrt{2\pi}}\exp\left[-\frac{\left(y-\mu_y\right)^2}{2\sigma_y^{2}}\right]$	(5)
Gumbel	$f(x)=\frac{1}{a}\exp\left[-\frac{\left(x-u^2\right)}{a}-\exp\left(-\frac{x-u}{a}\right)\right]$	(6)
	$a=\frac{\sqrt{6}S_x}{\pi}$	(7)
	$u=\bar{x}-0.5772a$	(8)
	$K_T=-\frac{\sqrt{6}}{\pi}\left\{0.5772+\ln\left[\ln\left(\frac{T}{T-1}\right)\right]\right\}$	(9)
	$X_T=\mu_X+\left(K_T\times\sigma_X\right)$	(10)

Table 1. (Continue) Probability Density Functions and calculation formulas

Log-Pearson Tip III	$$\log \bar{x} = \frac{\sum \log x}{N}$$	(11)
	$$\sigma_{\log x} = \sqrt{\frac{\sum\left(\log x - \log \bar{x}\right)^2}{N-1}}$$	(12)
	$$C_S = \left[\frac{N \times \sum\left(\log x - \log \bar{x}\right)^3}{(N-1)\times(N-2)\times\left(\sigma_{\log x}\right)^3}\right]$$	(13)
	$$\log x = \log \bar{x} + k \times \sigma_{\log x}$$	(14)

2.3. Synthetic unit hydrographs

Flood calculations are performed using synthetic unit hydrograph methods. For this purpose, various synthetic methods such as the DSI Synthetic Unit Hydrograph, the Mockus Synthetic Unit Hydrograph Method, and the Synder Synthetic Unit Hydrograph Method can be utilized. In this study, the physical characteristics of the study area were first determined using maps created in a GIS environment. The calculation process consists of three main steps. In the first step, precipitation values representing the studied watershed were calculated for various return periods. In the second step, a watershed-specific unit hydrograph was created using the physical characteristics of the watershed and dimensionless unit hydrograph coordinates. Finally, based on these data, flood peak values were calculated. The dimensionless unit hydrograph coordinates used in creating the hydrographs are presented in Table 2, and the details of these calculation steps are explained in the following sections.

Table 2. Dimensionless unit hydrograph coordinates

T / T_p	Q / Q_p	T / T_p	Q / Q_p	T / T_p	Q / Q_p
0.0	0.000	1.0	1.000	2.4	0.180
0.1	0.015	1.1	0.980	2.6	0.130
0.2	0.075	1.2	0.920	2.8	0.098
0.3	0.160	1.3	0.840	3.0	0.075
0.4	0.280	1.4	0.750	3.5	0.036
0.5	0.430	1.5	0.660	4.0	0.018
0.6	0.600	1.6	0.560	4.5	0.009
0.7	0.770	1.8	0.420	5.0	0.000
0.8	0.890	2.0	0.320		
0.9	0.970	2.2	0.240		

2.3.1. DSI synthetic unit hydrograph method

The DSI synthetic unit hydrograph Method is used for drainage areas up to 1000 km². For larger drainage areas, these areas are divided into smaller units, each less than 1000 km², to generate unit hydrographs [12]. Additionally, although the DSI synthetic unit hydrograph Method is recommended for application when T_p > 2 hours, it is not applied for areas smaller than 1 km². The catchment area (A) is determined using topographic maps. Then, the longest branch of the river is measured from the map (L), and the distance between the projection of the drainage area center onto the longest river branch and the project section is determined (L_c).

Firstly, the harmonic slope calculation of the land is required. For this purpose, starting from the river source and following the project section, elevations and distances are recorded. The entire length is segmented into ten equal parts, and the harmonic slope is determined accordingly. Basin harmonic gradient,

$$S = \left(\frac{10}{\sum \frac{1}{\sqrt{s}}} \right)^2 \tag{15}$$

Basin parameter,

$$E = \frac{L \times L_c}{\sqrt{S}} \tag{16}$$

Once the catchment area and basin parameters are determined, the Rain productivity (q_p) is calculated using Equation 17:

$$q_p = \frac{414}{A^{0.225} \times E^{0.16}} \tag{17}$$

q_p represents the discharge per unit km² of the rainfall area at the peak of the flood hydrograph, generated by a two-hour rainfall event that produces 1 mm of runoff over the basin.
The unit hydrograph peak discharge, Q_p (m³/s/mm):

$$Q_p = A \times q_p \times 10^{-3} \tag{18}$$

Unit hydrograph volume, V_b (m³):

$$V_b = A \times h_a \times 10^3 \tag{19}$$

The hydrograph duration (T, hours) and the hydrograph rise time (T_p, hours) are given in Equations 20 and 21, respectively.

$$T = 3.65 \frac{V}{Q} \tag{20}$$

$$T_p = \frac{T}{5} \tag{21}$$

After following the aforementioned procedure, the 24-hour rainfall-duration-return periods are multiplied by the number of pluviographs and the maximization factor (1.13). The adjusted rainfall values obtained are then used to determine the excess rainfall coefficients (h). The runoff coefficient is calculated using Equation 22.

$$h = \frac{\left(P - 0.2S\right)^2}{\left(P + 0.8S\right)} \tag{22}$$

Finally, the flood discharges are calculated by multiplying the peak discharge by the runoff coefficients determined separately for each return period (Equation 23).

$$Q = h \times Q_p \tag{23}$$

The Q_p and T_p values of the unit hydrograph are scaled using the dimensionless unit hydrograph coordinates to obtain the DSI synthetic unit hydrograph coordinates specific to the basin. The dimensionless unit hydrograph coordinates are provided in Table 2.

2.3.2. Mockus unit hydrograph method

In the Mockus method, hydrographs are triangular in shape, making them preferable due to their computational and graphical simplicity [13]. This method can be applied in regions where no streamflow gauging station is available or where long-term recorded data are lacking. The Mockus method is suitable for drainage basins with a collecting time (T_c) of less than 30 hours. The necessary parameters and procedural steps for generating a unit hydrograph using the Mockus method are presented below.

$$T_c = 0.00032 \times \frac{L^{0.77}}{S^{0.385}} \tag{24}$$

where T_c = Collecting Time (hours), L = Stream length (m), S = Harmonic slope

After determining the collecting time (T_c) based on stream length and harmonic slope, Precipitation time (D) is calculated using Equation 25:

$$D = 2\sqrt{T_c} \tag{25}$$

Then, the rise time of the hydrograph (T_p) is calculated according to Equation 26:

$$T_p = (0.5 \times D) + (0.6 \times T_c) \tag{26}$$

Hydrograph descent time (T_r) is calculated according to Equation 27:

$$T_r = 1.67 \times T_p \tag{27}$$

Flood time (T_b) is expressed as the sum of the rise time of the hydrograph and hydrograph descent time:

$$T_b = T_p + T_r \tag{28}$$

The discharge, Q_p, generated by a 1 mm rainfall, can be calculated using the following relation:

$$Q_p = \frac{K \times A \times h_a}{T_p} \tag{29}$$

Here, K is the catchment coefficient. Istanbulluoglu et al., [14] investigated the K value for various basins of Türkiye and showed that it varies between 0.10-0.40.

After following the aforementioned procedure, the 24-hour rainfall-duration-return periods are multiplied by the number of pluviographs and the maximization factor (1.13). The adjusted rainfall values obtained are then used to determine the excess rainfall coefficients (h). The runoff coefficient is calculated using Equation 22. Finally, the flood discharges are calculated by multiplying the peak discharge by the runoff coefficients determined separately for each return period, as given in Equation 23. The Q_p and T_p values of the unit hydrograph are scaled using the dimensionless unit hydrograph coordinates to obtain the coordinates of the Mockus Synthetic Unit Hydrograph specific to the basin.

2.3.3. Snyder unit hydrograph method

This method was proposed by Snyder [15] and in this method, Snyder studied unit hydrographs of basins located in the high regions of the Appalachian Mountains in the United States, defining a standard unit hydrograph. By examining unit hydrographs of various basins in the U.S., Snyder developed the following formulas for the T_p rise time and Q_p peak discharge of the unit hydrograph:

$$T_p = 0.75 \times C_t \times \left(L \times L_c \right)^{0.3} \tag{30}$$

Here, T_p is the rise time, L is the stream length, L_c is the distance from the centroid of the catchment area to the catchment outlet, and C_t is a coefficient related to the watershed surface.
The relationship between the effective rainfall duration, T_r, and the shower time, T_p, is given in Equation 31:

$$T_r = \frac{T_p}{5.5} \tag{31}$$

The unit discharge at the peak point of the hydrograph (q_p) (L/s/km²/cm) is calculated using the equation.

$$q_p = \frac{276 \times C_p}{T_p} \tag{32}$$

Here, C_p is a coefficient dependent on the characteristics of the catchment area. To determine the unit hydrograph for the catchment, the catchment parameters (C_p and C_t) mentioned above must be known. Table 3 shows the values of the relevant parameters used in the literature.

Table 3. Coefficient values related to the surface for the Snyder method [16]

Soil Type	C_t	C_p
Sandly	1.65	0.56
Bog	1.50	0.63
Clayey or rocky	1.35	0.69

Finally, the unit hydrograph peak discharge (m³/s/cm):

$$Q_p = A \times q_p \times 10^{-3} \tag{33}$$

The unit hydrograph peak discharge (m³/s/cm) is calculated from the formula. The obtained values represent the discharge corresponding to a 1 cm flow height. After following the aforementioned procedure, the 24-hour rainfall-duration-return periods are multiplied by the number of pluviographs and the maximization factor (1.13). The adjusted rainfall values obtained are then used to determine the excess rainfall coefficients (h). The runoff coefficient is calculated using Equation 23. Finally, the flood discharges are calculated by multiplying the peak discharge by the runoff coefficients determined separately for each return period, as given in Equation 24.

The Q_p and T_p values of the unit hydrograph are multiplied by the dimensionless unit hydrograph coordinates of the synthetic method to obtain the coordinates of the Snyder Synthetic Unit Hydrograph specific to the basin.

3. Result and Discussion

In this study, frequency analysis was performed using the largest daily (24-hour) rainfall values of the current year from the Sarıyer meteorological station (Figure 2), and the distribution function that best fits the sample distribution was selected. Daily maximum rainfall values for various return periods (T = 2, 5, 10, 25, 50, 100) were calculated. The extreme rainfall values for all probability functions at different return periods are summarized in Table 4 and presented in Figure 3. For short return intervals (T = 2, 5 years), the Normal distribution provides the highest extreme rainfall values, while for relatively long return intervals (T = 10, 25, 50, 100 years), the Log-Pearson Type III distribution generates the highest rainfall values.

Table 4. Extreme distribution of daily maximum precipitation

PDF	Return Periods (year)					
	2	**5**	**10**	**25**	**50**	**100**
Normal	62.80	85.24	96.95	109.48	117.56	124.80
Log-Normal	57.58	81.12	96.75	116.82	131.93	147.13
Gumbel	58.44	82	97.63	117.34	131.96	146.50
Log-Pearson Tip III	56.73	80.45	97.82	121.17	140.57	160.49

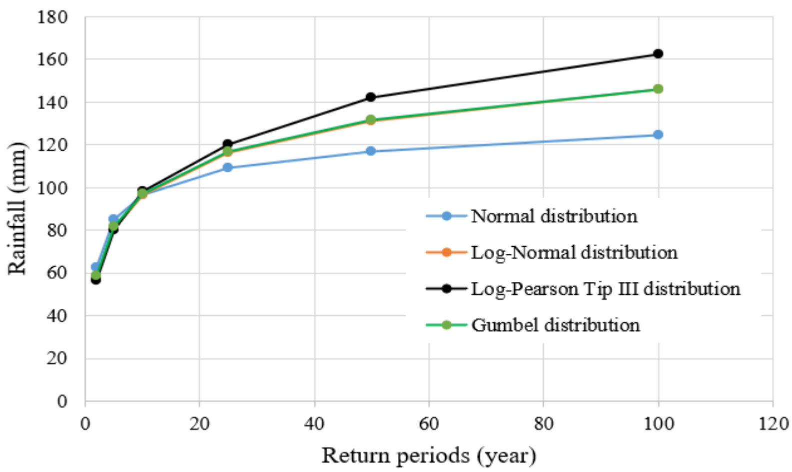

Figure 3. Extreme distribution of daily maximum precipitation

Many scientific studies in the literature have emphasized that the Log-Pearson Type III distribution should be used in flood discharge calculations [17-18]. Additionally, when compared to other probability distribution functions, the rainfall values obtained with the Log-Pearson Type III distribution are higher, and since floods are extreme events, the extreme rainfall values derived from this method have been used in discharge calculations.

As mentioned above, the basin unit hydrograph was obtained with the help of the basin's physical characteristics and the dimensionless unit hydrograph coordinates. Below, the physical characteristics of the basin that were initially identified, along with the magnitudes calculated using these characteristics, are presented (Table 5).

Table 5. Numerical values of study basin

Watershed Characteristics	Result
Watershed Area (km^2)	A= 10
Watershed minimum height (m)	2
Watershed maximum height (m)	234
Watershed mean height (m)	109.5
Watershed Direction	South, Southeast
Watershed longest flow path (m)	L= 6515
Centroidal longest flow path (m)	L_c = 2230

After the physical characteristics of the basin were determined in the ArcGIS 10.8 environment, the parameters required for the DSI synthetic unit hydrograph method were calculated as provided in Section 2.3.1 and are presented in Table 6.

Table 6. DSI synthetic method calculation table

Parameters	Calculation	Value
Harmonic slope	$\sqrt{S} = 10 / \sum (1/S)$	0.0197
Basin parameter	$E = L*L_c / \sqrt{S}$	103.43
Rain productivity	$q_p = 414/(A^{0.225}*E^{0.16})$	117.39
Peak discharge	$Q_p = A*q_p*10^{-3}$	1.174
Unit volume	$V_b = A*h_a*10^3$	10000
Hydrograph duration	$T=(3.65V_b/Q_p)/3600$	8.64
Hydrograph rise time	T_p	1.728

After determining the physical characteristics of the basin and the parameters for the DSI synthetic method, the 24-hour rainfall repetitions, pluviograph factor, precipitation area adjustment coefficient, and maximization value were adjusted. For this process, the final multiplication factor of 1.13 was applied to the current rainfall values to obtain the 24-hour adjusted rainfall values (Table 7). Then, using the 24-hour adjusted rainfall values, the excess rainfall coefficients (h) was calculated as given in Equation 22. Flood discharge values were obtained by multiplying the runoff coefficients with the peak discharge values for different return periods (Table 7).

Table 7. DSI method flood discharge calculation

	Return Periods (year)					
	2	5	10	25	50	100
Log-Pearson Tip III Rainfall Value	56.73	80.46	97.82	121.17	140.57	160.49
Final multiplication factor (1.13)	64.10	90.92	110.54	136.92	158.84	181.35
Excess rainfall coefficients (h)	2.21	9.47	17.19	29.99	42.31	56.22
Flood discharge (m^3/s)	2.498	11.083	20.340	34.546	51.002	67.443

The final obtained values of Q_p: 1.174 $m^3/s/mm$ and T_p: 1.728 hours were multiplied by the dimensionless unit hydrograph coordinates (Table 2) to derive the unit hydrograph for the stream (Figure 4a).

T_c is calculated by substituting the values of L (Watershed longest flow path) and S (harmonic slope) into the Equation 24 according to the Mockus method.

$T_c = 0.00032 * (6515^{0.77}/0.0197^{0.385}) = 1.254$ hour

The value of D is calculated by substituting T_c into the Equation 25:

$D = 2 * 1.254^{0.5} = 2.24$ hour

T_p is calculated by substituting the values of D and T_c into the Equation 26:

$T_p = 0.5 * 2.24 + 0.6 * 1.254 = 1.872$ hour

The values of T_r and T_b are calculated by substituting H (1.67 constant) and T_p into the Equation 27 to obtain T_r, and then substituting T_p and T_r into the Equation 28 to calculate T_b.

$T_r = 1.67 * 1.872 = 3.126$ hour

$T_b = 1.872 + 3.126 = 4.998$ hour

The value of Q_p is calculated by substituting the values of K, A and h into the Equation 29:

$Q_p = (0.208 * 10 * 1)/1.872 = 1.111\ m^3/s$

After determining the peak discharge, the 24-hour maximum rainfall values for different return periods and the excess rainfall coefficients were calculated (Table 8). As given in Equation 23, the peak discharge of the unit hydrograph multiplied by the flow coefficient resulted in the calculation of flood discharge values for different return periods, which are presented in Table 8.

Table 8. Mockus method flood discharge calculation

	Return Periods (year)					
	2	**5**	**10**	**25**	**50**	**100**
Log-Pearson Tip III Rainfall Value	56.73	80.46	97.82	121.17	140.57	160.49
Final multiplication factor (1.13)	64.10	90.92	110.54	136.92	158.84	181.35
Excess rainfall coefficients (h)	2.21	9.47	17.19	29.99	42.31	56.22
Flood discharge (m^3/s)	2.362	10.479	19.231	32.662	48.221	63.766

The final obtained values of Q_p: 1.111 $m^3/s/mm$ and T_p: 1.872 hours were multiplied by the dimensionless unit hydrograph coordinates (Table 2) to derive the unit hydrograph for the stream (Figure 4b).

For the Snyder method, as given in Equation 30, T_p (time to peak) is calculated as the rise time.

$T_p = 0.75 * 1.65 * (6.51 * 2.23)^{0.3} = 2.76$ hour

Using Equation 31, T_r is calculated:

$T_r = 2.76/5.5 = 0.55$ hour

According to Equation 32, the peak discharge per unit area of the standard unit hydrograph is calculated in units of ($l/sec/km^2/mm$):

$q_p = 276 * 0.56/2.76 = 56\ l/sec/km^2/mm$

Then, the discharge value at the flood peak is calculated using Equation 33:

$Q_p = 10* 56*10^{-3} = 0.560\ m^3/s/mm$

The final obtained values of Q_p: 0.560 $m^3/s/mm$ and T_p: 2.76 hours were multiplied by the dimensionless unit hydrograph coordinates (Table 2) to derive the unit hydrograph for the stream (Figure 4c).

Table 9. Snyder method flood discharge calculation

	Return Periods (year)					
	2	**5**	**10**	**25**	**50**	**100**
Log-Pearson Tip III Rainfall Value	56.73	80.46	97.82	121.17	140.57	160.49
Final multiplication factor (1.13)	64.10	90.92	110.54	136.92	158.84	181.35
Excess rainfall coefficients (h)	2.21	9.47	17.19	29.99	42.31	56.22
Flood discharge (m^3/s)	1.191	5.286	9.702	16.478	24.328	32.170

After determining the peak discharge, the 24-hour maximum rainfall values for different return periods and the flow coefficients were calculated (Table 9). As given in Equation 23, the peak discharge of the unit hydrograph multiplied by the excess rainfall coefficients resulted in the calculation of flood discharge values for different return periods, which are presented in Table 9.

Table 10 presents the flood discharge values calculated using different methods for various return periods. Additionally, Figure 4 illustrates the flood hydrographs computed for different methods and return periods. Furthermore, Figure 5 presents the flow values for different return periods obtained using different unit hydrograph methods and a representation of the maximum flood discharges observed for the 100-year recurring rainfall.

Table 10. Calculated flood discharge for different return periods

Methods	**Return Periods (year)**					
	2	**5**	**10**	**25**	**50**	**100**
DSI	2.498	11.083	20.340	34.546	51.002	67.443
Mockus	2.362	10.479	19.231	32.662	48.221	63.766
Snyder	1.191	5.286	9.702	16.478	24.328	32.170

When examining Figure 4 and Table 10, compared to the Snyder method, both the DSI and Mockus methods produced consistently higher peak discharges across all return periods. This similarity suggests not only comparable hydrograph shapes but also reinforces their reliability for small, forested catchments. In addition to the closeness of discharge values, these two methods also yield hydrographs with similar durations. In contrast to DSI and Mockus, the Snyder method generated substantially lower peak discharges and exhibited a more prolonged hydrograph response, likely due to its sensitivity to basin shape and longer time-to-peak assumptions. Furthermore, these discharges align with expectations for a small forest-dominated watershed of approximately 10 km^2. The highest peak discharge obtained (Q_{max} = 67.44 m^3/s for the DSI method at a 100-year return period) corresponds to an average unit discharge of ~6.74 $m^3/s/km^2$. This value is within the range reported in the literature for similar basins in Türkiye, especially those located in humid to semi-humid climates [5, 6]. Furthermore, the lower discharges produced by the Snyder method can be attributed to its sensitivity to shape parameters and its assumption of a longer time to peak. The close agreement between the DSI and Mockus results strengthens their applicability in small, forested catchments and confirms the hydrological plausibility of the computed discharges within the adopted methodological framework.

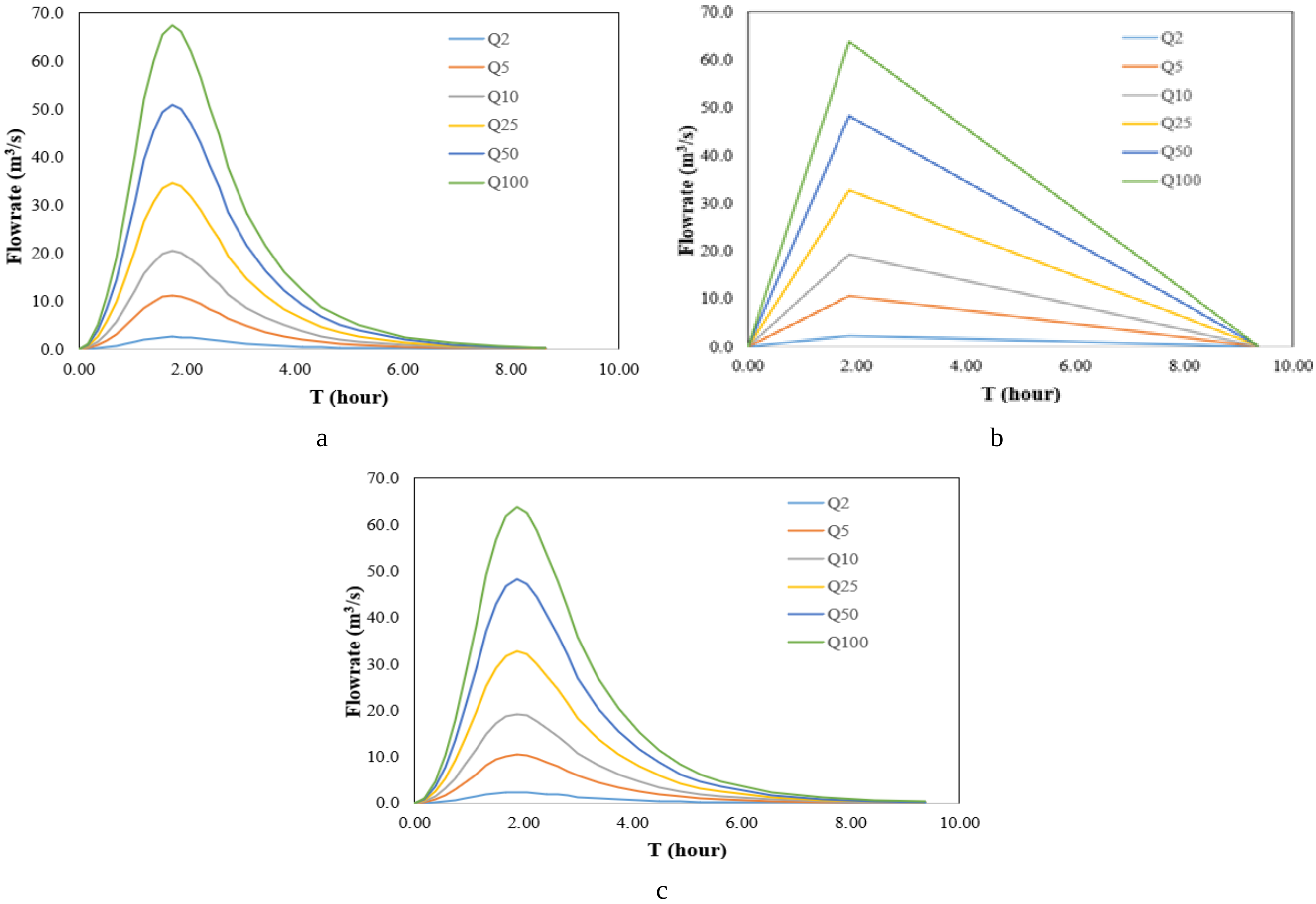

Figure 4. Various synthetic unit hydrograph methods and flood hydrographs for return periods: a) DSI Method, b) Mockus Method, c) Snyder Method (The DSI and Mockus methods show higher peak discharges and shorter durations compared to the Snyder method)

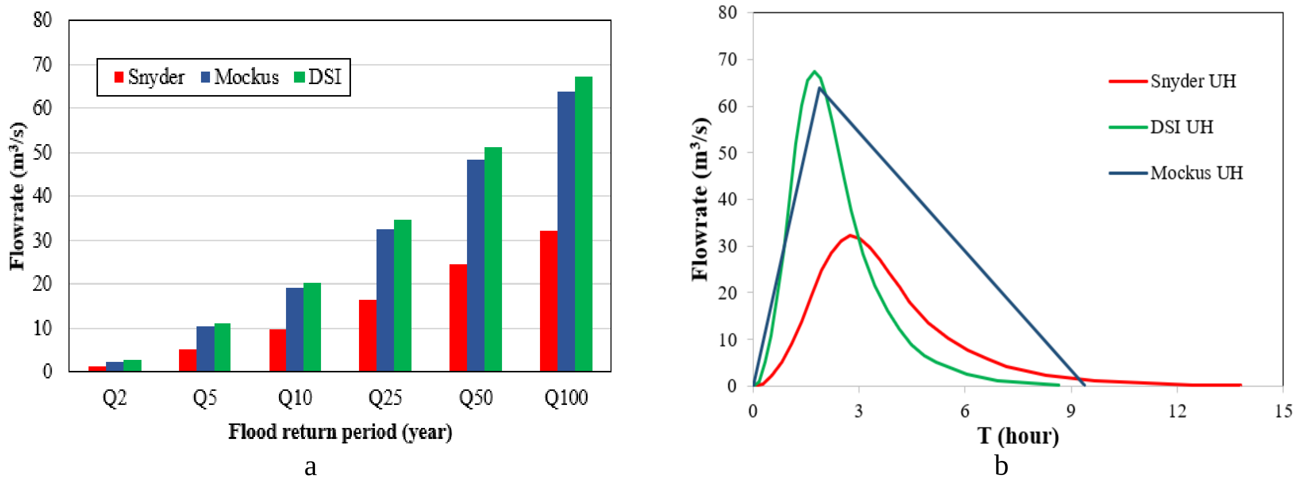

Figure 5. Comparison of flood discharges: a) DSI, Mockus, and Snyder methods for various return periods (The DSI method consistently produces the highest discharges across all return periods) b) Synthetic unit hydrographs for a 100-year return period (Snyder method results in a longer hydrograph duration and lower peak compared to DSI and Mockus methods)

In summary, the findings of the presented study are consistent with recent research highlighting the importance of method selection based on basin characteristics. Mukherjee et al. (2024) showed that deterministic methods are effective for small, forested headwater catchments, while other approaches perform better in larger basins [22]. Aziz et al. (2025) [23] emphasized statistical methods for urban flood planning, and Saplıoğlu (2025) [24] demonstrated that optimization techniques can enhance model accuracy. These studies support the conclusion that the DSI and Mockus methods are particularly reliable for flood estimation in small, ungauged, forested basins, such as the one examined in this study.

Given the destructive nature of floods as extreme hydrological events, it is essential to utilize the most severe hydrograph obtained in flood modeling studies. Accurately generated precipitation data and hydrographs with high-resolution values play a critical role in areas such as flood risk management, drainage design, infiltration assessment, and the long-term sustainability of urban infrastructure systems [19-21]. Accordingly, this study developed hydrographs that effectively represent watershed-scale rainfall-runoff relationships, which are fundamental inputs for the creation of flood inundation and water depth maps.

On the other hand, there are many uncertainties in hydrological modeling of ungauged basins. The main ones are potential errors in rainfall data—specifically for the application of one station—statistical uncertainty of extreme rainfall distributions that were fitted, and errors in land use classification due to satellite resolution or seasonality. In addition, empirical coefficients used for synthetic unit hydrograph methods, which are occasionally borrowed from other basins, may not be representative of local conditions. While these uncertainties are not precisely quantified in this study, they need to be considered when evaluating the results and planning future research.

4. Conclusion

This study evaluated three synthetic unit hydrograph methods—DSI, Mockus, and Snyder—for estimating flood discharges in a small, forest-dominated ungauged sub-basin in Istanbul. Among these, the DSI and Mockus methods yielded consistently higher and more conservative discharge values, aligning closely with each other and demonstrating suitability for hydrological applications in similar catchments. Their reliance on physically-based parameters rather than empirical coefficients enhance their practical utility, particularly in data-scarce environments.

While the selected methods performed robustly, attention must be paid to uncertainties such as limitations in rainfall measurement, classification errors in land use data, and assumptions inherent to empirical coefficients. These factors, although not explicitly quantified in this study, underscore the importance of further calibration and sensitivity analyses in future research.

The outcomes of this work offer a strategic foundation for advancing flood risk assessment and infrastructure planning in other ungauged, forested urban basins—especially those facing intensified challenges from rapid urbanization and climate variability.

5. Author Contribution Statement

Author 1 contributed to the idea, design and literature review, evaluation of the results, could be reworded as of the manuscript, and reviewed the manuscript for language accuracy and overall coherence.

6. Ethics Committee Approval and Conflict of Interest

There is no need to obtain ethics committee permission for the prepared article. There is no conflict of interest with any person/institution in the prepared article.

7. Ethical Statement Regarding the Use of Artificial Intelligence

No artificial intelligence-based tools or applications were used in the preparation of this study. The entire content of the study was produced by the authors in accordance with scientific research methods and academic ethical principles.

8. References

[1] F. Binici and T. Aksoy, “Şehirleşmenin Taşkın Üzerindeki Etkisi,” *GSI J. Serie C: Advancements Inf. Sci. Technol.*, vol. 5, no. 1, pp. 64–76, 2022.

[2] T. Akkuş, “Doğal Afetlerin Toplumsal Tarihe Etkileri Üzerine Yerel Bir Örnek: 1931–1941 Döneminde Edirne ve Çevresindeki Taşkinlar ve Sonuçları,” *Uludağ Univ. J. Soc. Sci.*, vol. 24, no. 44, pp. 69–96, 2023.

[3] Z. P. McEachran, J. Kietzmann, and M. Johnston, “Parsimonious streamflow forecasting system based on a dynamical systems approach,” *J. Hydrol.*, vol. 641, 2024.

[4] O. Sönmez, M. Öztürk, and E. Doğan, “İstanbul derelerinin taşkın debilerinin tahmini,” *Sakarya Univ. J. Sci.*, vol. 16, no. 2, pp. 130–135, 2012.

[5] A. A. Kumanlıoğlu and S. B. Ersoy, “Akım gözlemi olmayan havzalarda taşkın akımlarının belirlenmesi: Kızıldere Havzası,” *DEU Eng. Sci. J.*, vol. 20, no. 60, pp. 890–904, 2018.

[6] B. B. Bantchina and K. S. Gündoğdu, “Watershed Characteristics and Synthetic Unit Hydrographs Determination using Geographical Information Systems,” *J. Biol. Environ. Sci.*, vol. 15, no. 45, pp. 27–34, 2021.

[7] P. Dutta and S. Deka, “Reckoning flood frequency and susceptibility area in the lower Brahmaputra floodplain using geospatial and hydrological approach,” *River*, vol. 2, no. 3, pp. 384–401, 2023.

[8] U. Ahad, U. Ali, M. Inayatullah, and A. R. Shah, “Flood Frequency Analysis: A Case Study of Pohru River Catchment, Kashmir Himalayas, India,” *J. Geol. Soc. India*, vol. 98, no. 12, pp. 1754–1760, 2022.

[9] A. I. Shah and N. D. Pan, “Evaluation of probability distribution methods for flood frequency analysis in the Jhelum Basin of North-Western Himalayas, India,” *Cleaner Water*, vol. 2, 2024.

[10] S. Malik and S. C. Pal, “Potential flood frequency analysis and susceptibility mapping using CMIP5 of MIROC5 and HEC-RAS model: A case study of lower Dwarkeswar River, Eastern India,” *SN Appl. Sci.*, vol. 3, no. 1, 2021.

[11] N. Usul, *Engineering Hydrology*, Ankara: ODTÜ Basımevi, 2001.

[12] I. Gevrek and A. Irvem, “Antakya’da taşkına neden olan yan derelerde hidrograf analizi ile taşkın tahmini,” *Mustafa Kemal Univ. J. Agric. Sci.*, vol. 26, no. 3, pp. 533–542, 2016.

[13] Y. Koca, “Rize iyidere alt havzası ikizdere kesiti için birim hidrografın belirlenmesi,” Uzmanlık Tezi, T.C. Orman ve Su İşleri Bakanlığı, Ankara, 2014.

[14] A. Istanbulluoglu, F. Konukcu, and I. Kocaman, “Precise determination of Turkish spillway sizes from synthetic unit hydrographs to prevent flood damage,” *Acta Agric. Scand., Sect. B - Soil Plant Sci.*, vol. 54, no. 3, pp. 114–120, 2004.

[15] F. F. Snyder, “Synthetic unit hydrographs,” *Trans. Am. Geophys. Union*, vol. 19, pp. 447–454, 1938.

[16] H. Çelik, “Sel Kontrolünde Hidroloji,” *ÇEM Sel Kontrolü Semineri*, Afyonkarahisar, 2012.

[17] O. Sönmez, T. Hırca, and F. Demir, “Akım Ölçümü Olmayan Nehirlerde Farklı Yağış Akış Modelleri ile Tekerrürlü Taşkın Debisi Hesabı: Mudurnu Çayı Örneği,” in *Proc. 5th Int. Symp. Innov. Technol. Eng. Sci.*, Baku, Azerbaijan, pp. 2017, Sep. 29–30.

[18] M. E. Yurdakul, “Güney Sapanca Havzası taşkın yayılım haritalarının modellenmesi: Keçi Deresi örneği,” M.S. thesis, Sakarya Univ., Inst. Nat. Sci., Sakarya, 2019.

[19] K. Gezici, E. Kesgin, and H. Agaccioglu, “Hydrological assessment of experimental behaviors for different drainage methods in sports fields,” *J. Irrig. Drain. Eng.*, vol. 147, no. 9, 2021.

[20] K. Gezici and S. Şengül, “Estimation and analysis of missing temperature data in high altitude and snow-dominated regions using various machine learning methods,” *Environ. Monit. Assess.*, vol. 195, no. 4, 2023.

[21] B. Çirağ and M. Firat, “Two-dimensional (2D) flood analysis and calibration of stormwater drainage systems using geographic information systems,” *Water Sci. Technol.*, vol. 87, no. 10, pp. 2577–2596, 2023.

[22] S. Mukherjee *et al.*, “A watershed-scale multi-approach assessment of design flood discharge estimates used in hydrologic risk analyses for forest road stream crossings and culverts,” *J. Hydrol.*, vol. 632, Art. no. 130698, 2024.

[23] A. Q. A. B. A. Aziz *et al.*, “Estimation of flood frequency using statistical method: river basin for Sungai Jijan Malaysia,” *IOP Conf. Ser.: Earth Environ. Sci.*, vol. 1453, Art. no. 012053, 2025.

[24] K. Saplıoğlu, "Calibration of Linear Muskingum Model Coefficients and Coefficient Parameters Using Grey Wolf and Particle Swarm Optimization," *Water Resour. Manage.*, vol. 39, pp. 999–1014, 2025.